Mem. S.A.It. Suppl. Vol. 24, 85

Memorie della
Supplementi

Solar carbon monoxide: poster child for 3D effects

T.R. Ayres[1], J.R. Lyons[2], H.-G. Ludwig[3], E. Caffau[3], and S. Wedemeyer-Böhm[4]

[1] Center for Astrophysics & Space Astronomy, University of Colorado, Boulder, CO 80309, USA e-mail: Thomas.Ayres@Colorado.edu
[2] Dept. of Earth and Space Sciences, University of California, Los Angeles, CA, USA
[3] Zentrum für Astronomie der Universität Heidelberg, Heidelberg, Germany
[4] Institute of Theoretical Astrophysics, University of Oslo, Oslo, Norway

Abstract. Photospheric infrared (2–6 μm) rovibrational bands of carbon monoxide (CO) provide a tough test for 3D convection models such as those calculated using CO5BOLD. The molecular formation is highly temperature-sensitive, and thus responds in an exaggerated way to thermal fluctuations in the dynamic atmosphere. CO, itself, is an important tracer of the oxygen abundance, a still controversial issue in solar physics; as well as the heavy isotopes of carbon (^{13}C) and oxygen (^{18}O, ^{17}O), which, relative to terrestrial values, are fingerprints of fractionation processes that operated in the primitive solar nebula. We show how 3D models impact the CO line formation, and add in a second constraint involving the near-UV Ca II line wings, which also are highly temperature sensitive, but in the opposite sense to the molecules. We find that our reference CO5BOLD snapshots appear to be slightly too cool on average in the outer layers of the photosphere where the CO absorptions and Ca II wing emissions arise. We show, further, that previous 1D modeling was systematically biased toward higher oxygen abundances and lower isotopic ratios (e.g., $R_{23} \equiv {}^{12}$C/^{13}C), suggesting an isotopically "heavy" Sun contrary to direct capture measurements of solar wind light ions by the *Genesis* Discovery Mission. New 3D ratios for the oxygen isotopes are much closer to those reported by *Genesis,* and the associated oxygen abundance from CO now is consistent with the recent Caffau et al. study of atomic oxygen. Some lingering discrepancies perhaps can be explained by magnetic bright points. Solar CO demonstrates graphically the wide gulf that can occur between a 3D analysis and 1D.

Key words. Line: formation — Molecular processes — Sun: abundances — Sun: infrared — Sun: photosphere

1. Introduction

The so-called "Oxygen Crisis" (see, e.g., Ayres et al. 2006: APK) refers to a mismatch between contemporary recommended spectroscopic values of the solar oxygen abundance, at slightly below 500 parts per million (ppm) relative to hydrogen, and that favored by helioseismology, consistent with interior properties deduced from surface *p*-modes (more like 700 ppm; see Figure 1). But, there is a second — lesser known — crisis involving oxygen, specifically the heavy isotopes ^{17}O and ^{18}O. Comparing the oxygen isotope compo-

Send offprint requests to: T. Ayres

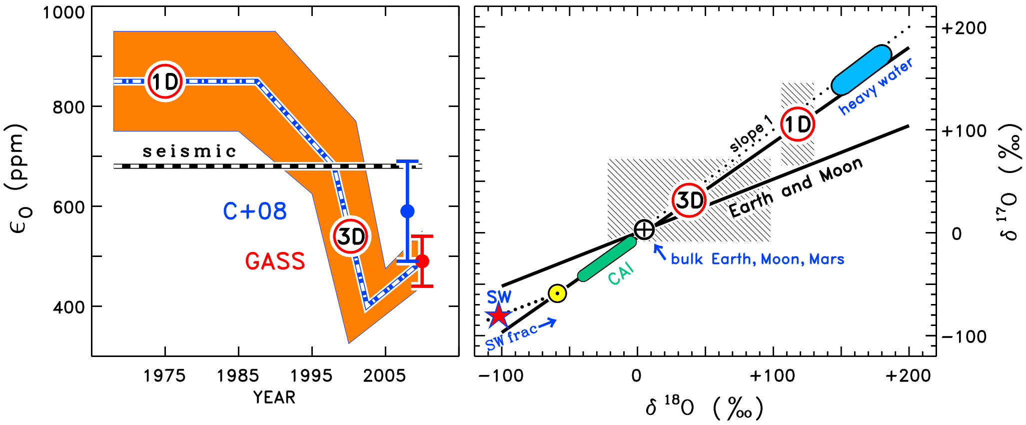

Fig. 1. *Left*— Trends of spectroscopic measurements of photospheric oxygen abundance (orange shaded area) over time (adapted from APK). Horizontal dashed line ("seismic") is value favored by helioseismology. Prior to 2000, 1D studies provided generally high oxygen abundances, well above seismic; but advent of 3D models dropped ϵ_O precipitously, far below seismic, inspiring so-called "Oxygen Crisis." While ϵ_O has recovered somewhat from its early-century lows, most recent recommended value (from Grevesse et al. 2010: GASS) still is inconsistent with seismic. Somewhat higher recent value of Caffau et al. (2008: C+08) also is illustrated. *Right*— 3-isotope plot comparing ^{17}O against ^{18}O. δ's are per mil offsets relative to standard isotopic ratios (with respect to ^{16}O) in ocean water (for geochemical reasons slightly isotopically lighter than bulk Earth). Red star is *Genesis* measurement of light ions captured from solar wind; Sun symbol accounts for correction due to wind fractionation processes. CAI refers to Ca-Al inclusions in chondritic meteorites; "heavy water," to extreme nebular metal grains in primitive chondrite Acfer 094 (adapted from McKeegan et al. [2011]: see ibid for details). Previous 1D and 3D spectroscopic estimates of photospheric ^{18}O are indicated, suggesting that the Sun, paradoxically, is isotopically heavier than Earth.

sition of the Sun to that of the planets and other Solar System objects opens a window onto the early evolution of the solar birth nebula, and especially the coagulation of the inner rocky planets like Earth. Previous measurements of photospheric oxygen isotopes, from infrared CO isotopomer absorption bands using 1D reference models, yielded surprisingly enriched heavy oxygen compared to terrestrial values (Harris et al. 1987; APK; e.g., $\delta\,^{18}$O $\sim$ +120 ‰ [per mil offsets relative to terrestrial standards[1]]): see Fig. 1. Application of an early-generation 3D convection model brought $\delta\,^{18}$O closer to terrestrial, but still positive and with uncomfortably large error bars (Scott et al. 2006: SAGS). By contrast, analysis of light ions directly captured from the solar wind by the *Genesis* Discovery Mission found photospheric values of –59 ‰ for both oxygen isotopes (McKeegan et al. 2011). Clearly, reconciling the *Genesis* and surface spectroscopy viewpoints would be desirable, both with regard to the oxygen abundance deficit, as well as the heavy isotope conundrum.

We therefore carried out a new, detailed study of photospheric CO and its isotopomers utilizing state-of-the-art 3D convection models calculated by the CO5BOLD consortium (Freytag et al. 2012). The results have been published in Ayres et al. (2013: A+13). Here we discuss several aspects of that study that are relevant to 3D modeling in general, and CO5BOLD in particular, including simulations of the Ca II H & K lines (3968 Å and 3933 Å, respectively) which were not presented in the earlier work (but indirectly played a key role). The mid-IR solar CO bands, in concert with near-UV Ca II, provide stringent tests of the thermal structure of a 3D model, because the two sets of diagnostics respond in opposite

[1] Vienna Standard Mean Ocean Water for the oxygen isotopes, and Vienna PeeDee Belemnite for carbon: see APK.

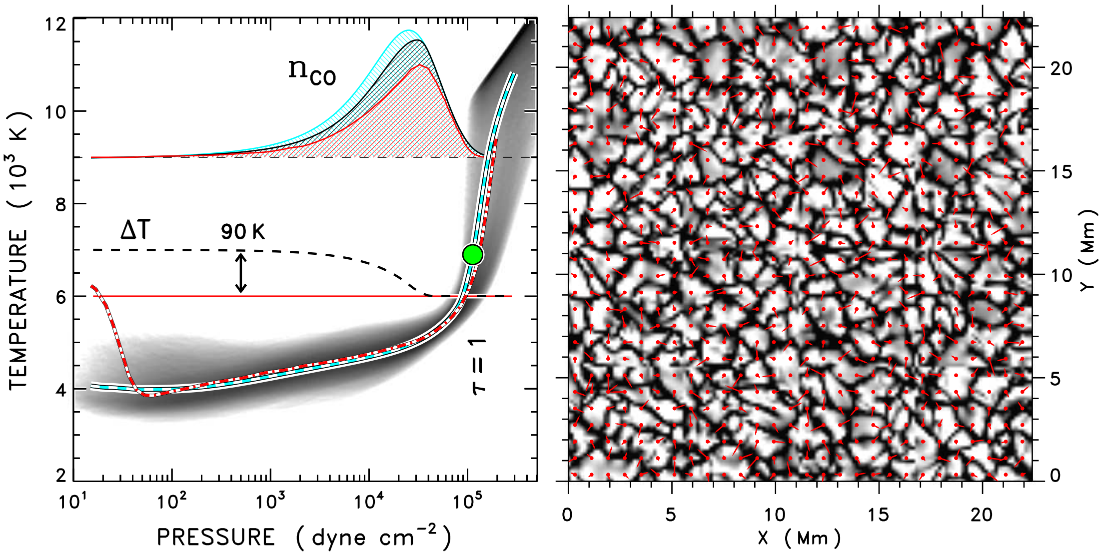

Fig. 2. *Right*— Velocity map of 3D "Baseline" model (16 independent snapshots arrayed together for display purposes): light= upflows; dark= downflows; red arrows= horizontal components; gray scale saturates at ±2 km s^{-1}. *Left*— Blue dashed curve is 3D temperature profile averaged over surfaces of constant pressure; red dot-dashed is FALC 1D model, slightly warmer than 3D average in upper layers (lower pressures). Gray shading illustrates power-density map of temperature variations. Green dot marks average pressure of white-light surface. Colored hatched curves are relative CO concentrations: blue– Baseline 3D model; black– 3D "MAX" (Baseline + 90 K in outer layers to match 1D average); red– 1D FALC. MAX and 1D have same average temperature profile, but former produces more CO, thanks to 3D fluctuations.

ways to the thermal fluctuations inherent in the convective flows.

2. Observations

For the CO part of the story, our approach was to synthesize profiles of CO parent lines ($^{12}C^{16}O$) with a given photospheric thermal model to derive an oxygen abundance appropriate for that specific model. We then applied that oxygen abundance to the weaker isotopomer lines, to infer the isotopic ratios.

The CO rovibrational transitions have a number of important advantages for such an analysis: (1) large isotopic frequency shifts, due to impact of the different molecular weights on the rotation-vibration properties; (2) durable molecule, with its 11 eV dissociation potential; prolific throughout much of the photosphere; (3) reasonably strong isotopomer lines thanks to the high abundance of CO; (4) thousands of potentially useful lines to resolve issues with, say, blends (in fact, most blends are with other CO lines, and can be readily identified through spectrum synthesis); and (5) wide range of excitation energies to gauge temperature effects. There is a big drawback, however: the molecular formation is very sensitive to temperature, and thus highly model-dependent.

The main CO bands — fundamental (Δv = 1) and first-overtone (Δv = 2) — fall in the thermal infrared (ω = 2150 cm^{-1} [4.6 μm] and ω = 4300 cm^{-1} [2.3 μm], respectively). They are fully captured in the excellent high-resolution ($\omega/\Delta\omega \sim 10^5$) atlas of the disk center IR spectrum, free of telluric contamination, from the 1990's *Shuttle*–borne *ATMOS* experiment (see APK).

The many potentially usable CO rovibrational features is good news compared with the only few lines sometimes available for atomic species in the visible (e.g., Caffau et al. [2008:

C+08] for O I); but is somewhat bad news in the 3D context, because a large number of target lines is computationally burdensome. We worked around this "embarrassment of riches" by "hybridizing" groups of several CO lines of similar excitation and line strength into single composite features of enhanced S/N and better defined continuum level. The approach is described in A+13.

A key part of any spectroscopic analysis is the underlying atomic data. For molecules like CO, transition frequencies and excitation energies are very accurately known, but the crucial oscillator strengths typically are not as well determined. We considered two such scales for this work: Goorvitch (1994: G94) and Hure & Roueff (1996: HR96). Ratios of these f-values display systematic deviations, including trends with $E_{\rm low}$, at the several percent level (see A+13 for details). Despite this, *within* either of the scales, there is almost exactly the same relative behavior of the isotopomer f-values with respect to the corresponding parents: systematically 2–4% below, depending on isotopomer, but independent of $E_{\rm low}$.

The subsequent discussion mainly will rely on a simple average of the G94 and HR96 f-values, which we call $\langle f \rangle$.

3. Analysis

We utilized a recent generation of CO5BOLD 3D convection models, specialized for the solar case. These reproduce key empirical constraints, such as absolute continuum intensities and limb darkening at visible wavelengths (Freytag et al. 2012; A+13). We chose sixteen snapshots from a fully relaxed CO5BOLD run (a majority subset of those used by C+08), sufficient for spatial/temporal averaging. A surface velocity map of the snapshots (butted together in a 4×4 grid for display) is shown in Figure 2; a white-light image would appear roughly similar. The 3D model has large temperature fluctuations in its outer layers, non-linearly impacting the highly temperature-sensitive molecules (and the near-UV Ca II resonance lines, as well). The average temperature profile of the "Baseline" 3D model in its high layers is systematically 90 K cooler than the FALC 1D reference stratification (Fontenla et al. 1993), used here for comparison.

3.1. Ca II wings

Given the apparent small, but conspicuous, temperature deficit of the Baseline 3D average relative to 1D, we carried out simulations of the extensive damping wings of the Ca II H & K lines mentioned earlier, which are well-known tracers of photospheric thermal structure (e.g., Ayres 1975). The Ca II wings arise in the same altitude range as the CO bands, but carry the opposite sensitivity to temperature fluctuations owing to the exponential response of the near-UV (Planckian) emissivities (see Ayres et al. 1986). We treated the wing radiation transport using a partial-coherent-scattering formalism, adapted to 3D, to account for density-dependent frequency-redistribution effects (Ayres 1975).

Synthesized H & K wing profiles are compared in Figure 3 with super-high spectral resolution disk-center scans from the McMath-Pierce FTS calibrated in absolute specific intensities (APK). The FALC 1D model was specifically designed to match the Ca II disk-center wing intensities, and our own simulations (not shown) verify that agreement. Interestingly, and perhaps significantly, the 90 K enhanced version of the Baseline 3D model ("MAX" variant) also shows excellent agreement with the Ca II wings; contrary to the Baseline model itself, which displays a small intensity deficit in the extreme inner wings (corresponding to the CO altitude range). Note, however, that because the uniform temperature enhancement is restricted to the higher altitudes, the far Ca II wings, reaching toward the continuum, are reproduced by both 3D variants.

Even with the good match to Ca II, we consider the 3D MAX variant to represent the outer limit of allowable temperature excursions, because the 3D Baseline model is a pure radiation-hydrodynamics (RHD) simulation with no allowance for the small-scale magnetic features that pepper the real Sun, even in the quietest areas, although with small covering fractions (perhaps only 5–10 % at

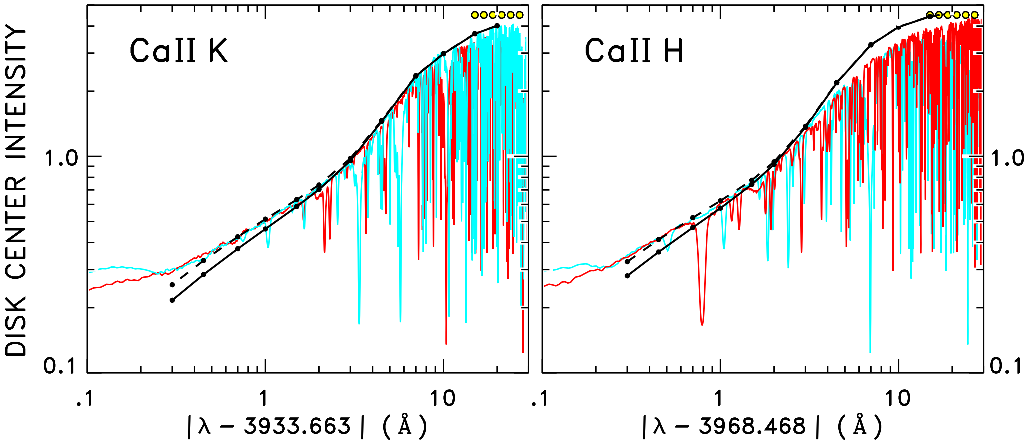

Fig. 3. 3D synthetic wing profiles for Ca II H & K calculated with Baseline model (solid curve) and MAX variant (dashed: 90 K enhanced in outer layers, only). In each panel, longwavelength (red) and shortwavelength (blue) disk-center wing intensities are over-plotted: sufficient line-free windows are available to compare with pure-wing simulations. 1D FALC Ca II wings would be indistinguishable from 3D MAX.

high altitudes). These so-called "flux tubes" are partially evacuated (owing to a balance between internal magnetic and external gas pressures) and tend to be hostile to density-friendly molecules, hence their appearance as "bright points" in G-band filtergrams (green wavelengths dominated by the CH molecule). The magnetic fibrils also display excess brightness in Ca II, so inclusion of these features would compensate for some of the temperature enhancement of the Baseline 3D model needed to replicate the Ca II wings. This was our motivation to describe the temperature-enhanced version of the Baseline 3D model as "MAX."

3.2. CO absorption bands

The detectable isotopomer lines all are low-excitation fundamental transitions. Unfortunately, the corresponding (same rotation-vibration transition) parents would be too strong for an abundance analysis. In fact only a relatively few unsaturated $^{12}C^{16}O$ fundamental lines cover the relevant $E_{\rm low} < 20,000\ {\rm cm}^{-1}$ range.

We thus also considered low-excitation parent overtone transitions, weak enough for reliable abundances, to map out any excitation-dependent trends over the same (low) energy range inhabited by the strongest isotopomers. The smaller sample of suitable fundamental transitions then served to compensate for any systematic offsets between $\Delta v = 1$ and $\Delta v = 2$ (which devolve partly from temperature effects but also systematic errors in the f-values).

Because we have several dozen parent CO "hybrid" lines, of differing absorption strength and excitation, we treated the common factor between them — the oxygen abundance[2] — as a "transfer standard." We did this by calculating the theoretical line strengths of each transition over a set of discrete oxygen abundances, then interpolating with the measured hybrid equivalent width (W_ω) to find the corresponding $\epsilon_{\rm O}$ (see A+13 for details concerning the spectrum synthesis). When displayed versus $E_{\rm low}$, we often found a slope of the $\epsilon_{\rm O}$'s, and usually also a separation between fundamental and overtone. As illustrated in Figure 4, the 1D model was most extreme in these respects, and incidentally also required the largest average oxygen abundance.

We repeated the experiment after slightly boosting the Baseline 3D temperatures uni-

[2] For simplicity, we assumed C/O= 0.5, based on independent assessments of the ratio (APK).

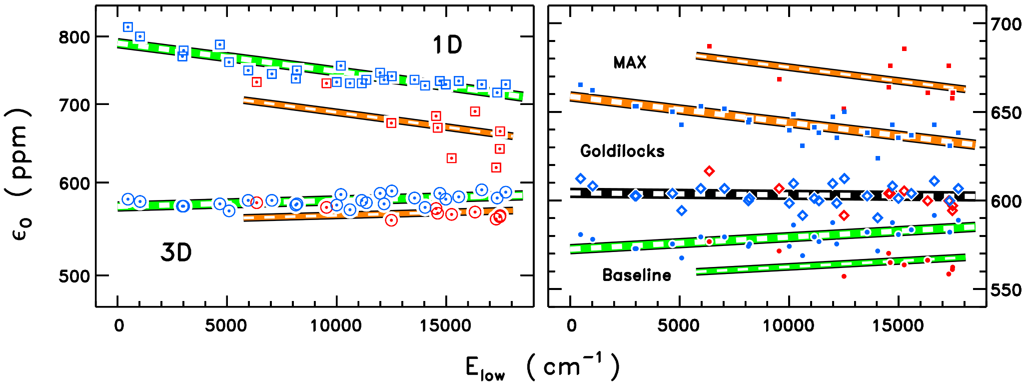

Fig. 4. *Left*— Circles represent oxygen abundances derived from individual parent CO lines using the Baseline 3D model and $\langle f \rangle$ scale. Red symbols are for fundamental transitions; blue, for first-overtone. Squares are values from the 1D FALC model, with same color-coding. Note "excitation slopes" and fundamental/first-overtone "separations," both much worse for 1D. Also note high ϵ_O's for 1D. *Right*— On expanded, linear scale; for three variants of the 3D model: "Baseline" (lower dots); "MAX" (upper small squares); and "Goldilocks" (middle diamonds: smaller T enhancement to force fundamental and first-overtone ϵ_O's to agree). Note that the excitation slopes and separations are opposite for Baseline and MAX, and the slope is nearly zero for Goldilocks (its separation is zero by design).

formly in the outer layers: for the MAX scenario, mentioned earlier, by the 90 K difference between 1D and 3D average temperature profiles (which incidentally also matches the Ca II wings, as noted earlier), and for the "Goldilocks" scenario, by a (smaller) ΔT needed to bring fundamental and overtone abundances into agreement (the specific offset depends on the f-value scale assumed). Resulting distributions of derived fundamental and overtone ϵ_O's are illustrated in Figure 5, for the $\langle f \rangle$ scale. Note that the Goldilocks variant (zero separation by design) also has the flattest excitation slope, not a foregone conclusion from simply forcing $\Delta v = 1$ and $\Delta v = 2$ to agree. Both characteristics (zero excitation slope, no separation) are desirable and would be considered positive indications that a model is compliant with the highly temperature sensitive CO molecules (see SAGS, APK).

The Goldilocks ΔT for the $\langle f \rangle$ scale is only $\sim$ 35 K above the Baseline model ($\Delta T \equiv 0$). If this represents a real difference, it might be a consequence of the limited frequency bins in the CO5BOLD runs[3]; or perhaps an indication of additional heating in the outer photosphere not accounted in the pure-RHD simulations (magnetic effects, high-frequency acoustic waves, etc.). Nevertheless, the excellent performance of the recent 3D models, even despite the approximations necessary to make the RHD tractable, is encouraging.

Findings of the oxygen analysis are depicted in Figure 5, for the three variants of the 3D model (Baseline, Goldilocks, and Max) and 1D. The main results, encapsulated in the 3D "bow-tie" and 1D "wedge,"[4] were derived for the $\langle f \rangle$ scale, but the corresponding Goldilocks results for G94 and HR96 are illustrated as well. The Goldilocks outcome depends on the specific oscillator strength scale, because the

[3] A dozen versus the tens of millions found in contemporary stellar 1D radiative equilibrium modeling; but, to be sure, the more recent 3D simulations find warmer photospheric temperatures than the earlier generation utilizing just a few frequency bins; which has led to improved agreement, for example, with visible continuum limb darkening.

[4] 1D also has a Goldilocks variant; but MAX and Baseline are the same by definition, so the bow-tie folds into a wedge.

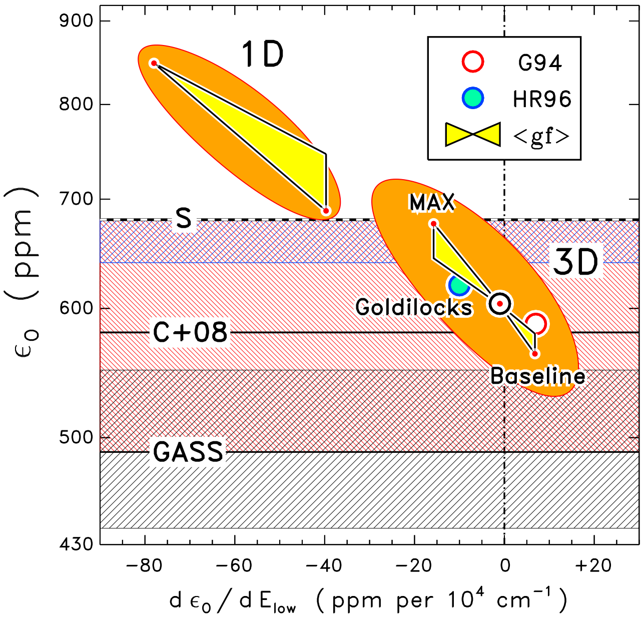

Fig. 5. Summary of oxygen abundances derived from model variants and different f-value scales, plotted versus excitation slope. "Bow-tie" for 3D was derived using $\langle f \rangle$ scale: results for Baseline model are at lower right, MAX at upper left; and Goldilocks in the middle. At each edge (and in middle), a small red dot marks the average ϵ_O derived from $\Delta v = 1$ parent lines; adjacent unmarked corner represents the average ϵ_O from $\Delta v = 2$: displacement indicates "separation" seen in Fig. 4. Large dots represent Goldilocks values derived for independent oscillator strength scales, according to the legend. Because of systematically opposite behavior of $\Delta v = 1$ and $\Delta v = 2$ f-values in the G94 and HR96 scales, the balance temperatures are somewhat different, thereby affecting the derived ϵ_O's. 1D model Baseline is at lower right of wedge. Like 3D, there is a (higher) Goldilocks ΔT to force fundamental and overtone to agree (point of wedge). However, excitation slope is steep and negative; unlike 3D Goldilocks for which the slope is nearly zero.

systematic, opposite separation of $\Delta v = 1$ and $\Delta v = 2$ f-values on the two scales impacts the balance ΔT, and thus the inferred highly model-dependent oxygen abundance.

3.3. C/O isotopic ratios

Final step was to take the oxygen abundances derived for each variant of the 3D and 1D models, together with the corresponding excitation slopes, and use this information to synthesize the isotopomer hybrids (specifically correcting the f-values to compensate for the fact that the excitation slope implies different oxygen abundances for different $E_{\rm low}$'s). We calculated profiles for seventeen hybrid features split among the isotopomers, for a discrete set of isotopic ratios relative to terrestrial standard values. The approach is illustrated in Figure 6. Note the slight convective blueshift of the CO isotopomer line shapes: it is about half the maximum ~600 m s^{-1} seen in visible Fe I and Fe II absorptions from the deep photosphere where the convective dynamics are more intense.

Figure 7 compares the derived offsets of the isotopomers relative to the standard isotopic ratios, as functions of $E_{\rm low}$ and W_ω, for the Goldilocks 3D model and $\langle f \rangle$ scale. Note that at least ^{13}CO and C^{18}O do not display any significant trends with excitation energy, presumably thanks to compensation for the apparent excitation slopes. Further, the dispersions within those two samples are consistent with the photometric noise in the *ATMOS* material, as suppressed by the hybridization process. For those two isotopomers, the observational S/N

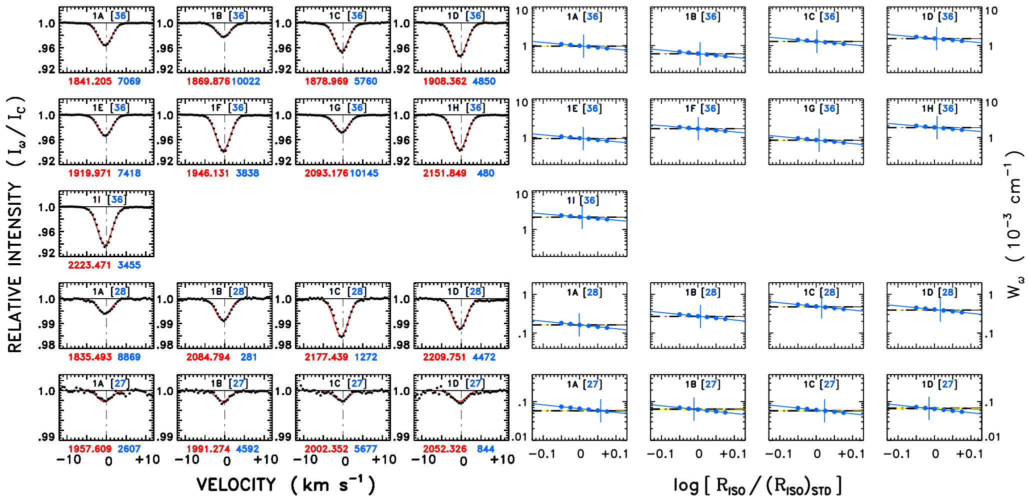

Fig. 6. *Left*— 3D synthetic line profiles, Goldilocks model for $\langle f \rangle$ scale, of isotopomer hybrids for standard terrestrial isotopic ratios: dots are observed lineshapes; thin red curves are calculated. Note slight convective blueshifts. *Right*— Calculated equivalent widths for a range of discrete offsets around standard values. Horizontal lines are observed W_ω's; intersection is inferred isotopic offset.

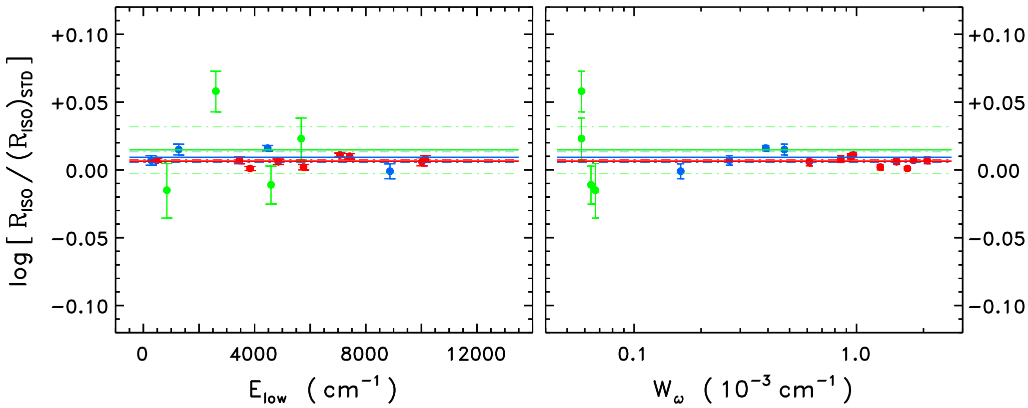

Fig. 7. Isotopic offsets from Fig. 6 vs. $E_{\rm low}$ and W_ω: red= ^{13}C; blue= ^{18}O; green= ^{17}O. Note that the isotopomers (all of $\Delta v = 1$ type) cover only a limited, lower range of $E_{\rm low}$, with minimal overlap with the parent fundamental sample. Overtone parent sample, on the other hand, fully covers the $E_{\rm low}$ range: motivation to include the $\Delta v = 2$ lines, and achieve agreement between fundamental and overtone via the Goldilocks ΔT. Note also extreme weakness of the C^{17}O features, even in highly collective hybrid form.

is not the limiting factor for deriving isotopic ratios. Conversely, for C^{17}O uncertainties in the line strengths are the major limitation.

4. Discussion

We derived isotopic ratios from our analysis of 3D solar CO corresponding to $\delta\,^{13}$C ~ -22 ‰, $\delta\,^{18}$O ~ -23 ‰, and $\delta\,^{17}$O ~ -42 ‰; much closer to *Genesis,* at least for the heavy oxy-

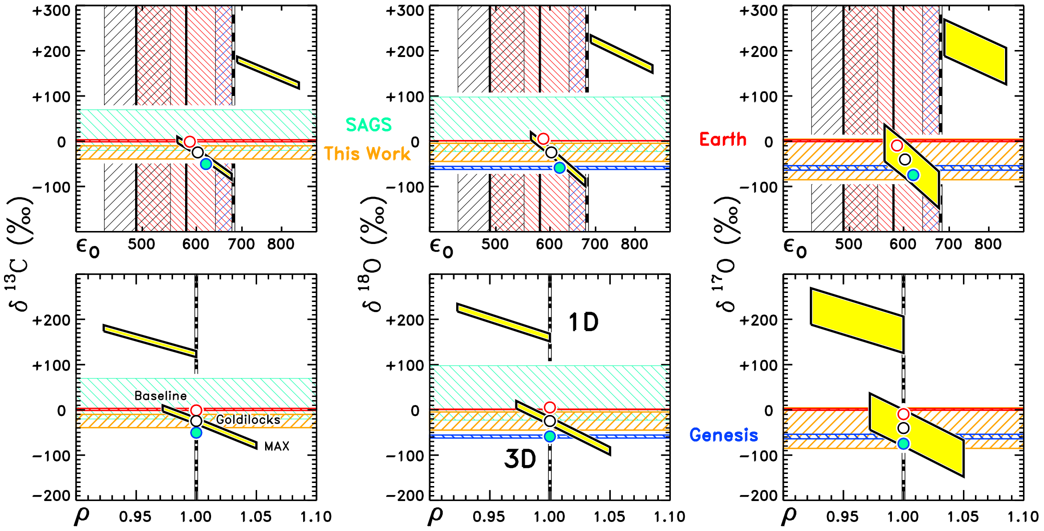

Fig. 8. Summary of isotopic findings. Per mil δ's relative to terrestrial are displayed vs. $\epsilon_{\rm O}$ in upper panels, and fundamental/overtone abundance ratio ("ρ"; $\rho = 1$ is Goldilocks constraint) in lower. Model variants are illustrated by shaded areas: vertical extents represent observational S/N. Large dots again show effect of different f-value scales for the three Goldilocks variants, with same coding as before. Orange hatching shows our preferred values; green hatching marks previous 3D results (SAGS); zero lines represent terrestrial ratios; and blue horizontal lines are for *Genesis.* Vertical shading in upper panels corresponds to horizontal shading in Fig. 5. Note that the 1D model favors oxygen-rich, isotopically heavy Sun. 3D favors a slightly oxygen-poor Sun, but isotopically lighter than Earth, more consistent with *Genesis.*

gens. These results are compared in Figure 8 with our 1D values and the previous 3D study of SAGS. (It should be noted that SAGS used an earlier generation of 3D models that likely was even cooler in the outer layers than our CO5BOLD snapshots, judging by the much lower abundances derived by those authors.) The new 3D values were based on the average of the G94 and HR96 f-values, and the several percent differences between the two constitute a major part of the systematic errors. In fact, if one turns the situation around and takes the *Genesis* $\delta\,^{18}$O at face value, 3D CO favors the HR96 scale. Some residual modilization issues also contribute. Namely, is Goldilocks truly the optimum model variant? And, what is the role played by magnetic bright points?

We can address the bright-point issue in a semi-quantitative way. If we assume that the small-scale magnetic elements contribute nothing to the CO equivalent widths, but radiate in the IR continuum just like the background atmosphere (e.g., 3D Baseline), then the calculated 3D CO W_ω's will be diminished by whatever the covering fraction of the bright points is in the high-altitude CO zone, say 10%. This implies that the derived fundamental and overtone $\epsilon_{\rm O}$'s will increase, depending on the slope of the W_ω–$\epsilon_{\rm O}$ relationship (which is different for $\Delta v = 1$ and $\Delta v = 2$: the power-law indices are about 0.9 and 1.4, respectively). For the 10% covering, the fundamental $\epsilon_{\rm O}$ would increase by about 60 ppm over the Baseline 3D value of 560 ppm, while the overtone $\epsilon_{\rm O}$ would increase by a smaller amount, 40 ppm, but on top of a higher base, 580 ppm. These increments provide a new $\epsilon_{\rm O}$ of 620 ppm for both fundamental and overtone, in other words, the desired Goldilocks balance (*but without any increase in the Baseline 3D temperatures*). The equivalent ΔT to reproduce the effect of the 10% "holes" in the CO zone is about 50 K, again similar for fundamental and overtone (but higher than the $\sim$ 35 K Goldilocks ΔT assuming no magnetic points, at least for the $\langle f \rangle$ scale). This demonstrates that the presence of small-scale CO-free 'spots' can replicate the effect of a uniformly hotter 3D atmosphere, but is not exactly equivalent because of the nonlinear, and different, responses of the fundamental and overtone lines.

As for the Ca II wings, the difference between the observed and Baseline 3D simulated intensities is about 10% for $|\Delta\lambda| \leq 1$ Å, corresponding to the altitudes of the main CO zone. If the hot spots cover 10% of the area at those altitudes[5], and add an extra 10% in intensity over the background atmosphere, then they must have a Ca II wing brightness contrast of ~ 2, certainly not unreasonable.

So, qualitatively, adding magnetic bright points into the picture could explain the CO bands and Ca II wing intensities simultaneously, if the hot spots had the correct properties, *without altering the Baseline 3D model.* It remains to be seen however, if a proper 3D R-MHD simulation of the photosphere would actually work out that way.

5. Conclusions

Beyond the scientific impact of the isotopomer results, a surprising aspect of Fig. 8, in hindsight, is the large disagreement between the 3D and 1D approaches. Since the isotopic abundances are expressed as *ratios* with respect to the parent abundances, ordinarily one anticipates that at least some cancellations will occur, rendering the final ratios much less model-dependent than, say, the derived absolute oxygen abundances (e.g., Fig. 5). However, for this particular problem and analysis approach, those mitigating effects apparently were not achieved for the 1D case. This is an additional example of the bad outcome that potentially can follow the cavalier use of a 1D model, even in a situation where the desired result is differentially determined, and presumed to be less sensitive to the 3D versus 1D dichotomy.

Several take-away points from our "forensic spectroscopy" of solar CO (and Ca II): (1) the parallel "Oxygen Crises" in abundance and isotopic ratios perhaps are not as severe as once thought, thanks to the new insights provided by 3D modeling; (2) the IR CO bands and near-UV Ca II wings can provide parallel, complementary tests of the thermal properties of a 3D model, especially if the influence of small-scale magnetic elements can be better quantified (recent work by, e.g., Sheminova [2012] and Henriques [2012], are steps in that direction); and (3) solar carbon monoxide in particular, and stellar molecules in general, have to be considered a poster child for the importance of 3D effects, and strong motivation to further advance the RHD (and R-MDH) modeling state-of-the-art for all cool stars.

[5] Magnetic flux tubes likely would be funnel shaped, with a larger cross section higher up (due to magnetic expansion), but a much smaller cross section in the deeper layers.

Acknowledgements. This work was supported by NSF grant AST–0908293. JRL thanks NASA Origins of Solar Systems and the Penn State Astrobiology Research Center. EC and HGL acknowledge financial support by the Sonderforschungsbereich SFB 881 "The Milky Way System" (subproject A4) of the German Research Foundation (DFG).

References

Ayres, T. R. 1975, ApJ, 201, 799
Ayres, T. R., Testerman, L., & Brault, J. W. 1986, ApJ, 304, 542
Ayres, T. R., Plymate, C., & Keller, C. U. 2006, ApJS, 165, 618 (APK)
Ayres, T. R., Lyons, J. R., Ludwig, H.-G., Caffau, E., & Wedemeyer-Böhm, S. 2013, ApJ, 765, 46 (A+13)
Caffau, E., Ludwig, H.-G., Steffen, M., et al. 2008, A&A, 488, 1031 (C+08)
Fontenla, J. M., Avrett, E. H., & Loeser, R. 1993, ApJ, 406, 319
Freytag, B., Steffen, M., Ludwig, H.-G., et al. 2012, J. Comp. Phys., 231, 919
Goorvitch, D. 1994, ApJS, 95, 535 (G94)
Grevesse, N., Asplund, M., Sauval, A. J., & Scott, P. 2010, Ap&SS, 328, 179 (GASS)
Harris, M. J., Lambert, D. L., & Goldman, A. 1987, MNRAS, 224, 237
Henriques, V. M. J. 2012, A&A, 548, A114
Hure, J. M., & Roueff, E. 1996, A&AS, 117, 561 (HR96)

McKeegan, K. D., Kallio, A. P. A., Heber, V. S., et al. 2011, Science, 332, 1528
Scott, P. C., Asplund, M., Grevesse, N., & Sauval, A. J. 2006, A&A, 456, 675 (SAGS)
Sheminova, V. A. 2012, Sol. Phys., 280, 83